

Reciprocal Beyond Diagonal Reconfigurable Intelligent Surface: Distributed Scattering Matrix Design and MIMO Beamforming via Fractional Programming and Manifold Optimization

Iván Alexander Morales Sandoval[✉], *Graduate Student Member, IEEE*,
 Marko Fidanovski[✉], *Graduate Student Member, IEEE*, Hyeon Seok Rou[✉], *Member, IEEE*,
 Giuseppe Thadeu Freitas de Abreu[✉], *Senior Member, IEEE*, Emil Björnson[✉], *Fellow, IEEE*.

Abstract—We consider the optimization of beyond diagonal reconfigurable intelligent surface (BD-RIS)-aided multi-user (MU) cell-free (CF)-massive multiple-input multiple-output (mMIMO) systems, where the propagation environment design achieved scattering matrix optimization is complemented by developing an efficient base station (BS) beamforming (BF) scheme that effectively exploits the latter “engineered” channel. In particular, we describe a fractional programming (FP) method, which based on the equivalent channel incorporating a reciprocal BD-RIS (RBD-RIS) parameterized by existing scattering matrix design methods, yielding the correspondingly optimized multiple-input multiple-output (MIMO) BF weights. The proposed approach decomposes the transmit (TX) beamformer into multiple sum-rate maximization (SRM) sub-beamformers, each satisfying an independent power-constraint, such that distributed MIMO-BF scenarios can be optimally handled. Although the proposed SRM-MIMO-BF framework is independent of the specific scattering matrix design, extending the BD-RIS-aided system model to the CF-mMIMO setting requires the design of a corresponding beamforming matrix. In this context, this work investigates the impact of beamforming in reconfigurable intelligent surface (RIS)-aided systems. Simulation results demonstrate that the proposed method for designing the MIMO-BF weights, when combined with the previously developed design of reciprocal BD-RIS (RBD-RIS) scattering matrices, outperforms existing BD-RIS-aided state-of-the-art (SotA) schemes employing existing MIMO-BF techniques, indicating that the whole contribution is more than the sum of the parts.

Index Terms—Beyond diagonal RIS, beamforming, fractional programming, sum-rate maximization.

I. INTRODUCTION

BEAMFORMING (BF) is an essential technique employed at either or both ends of modern wireless communications systems, which utilizes knowledge of the channel state to mitigate interference, enhance signal quality, add robustness, increase achievable rates, and improve the energy efficiency of the system. In turn, reconfigurable intelligent surfaces (RISs) are deployed to the environment itself, having similar effects as BF, but without requiring significant power and radio-frequency (RF) processing such as down-conversion, sampling, decoding, etc.

Unlike BF, which reacts to a given channel state, RISs fundamentally modify the propagation channel itself by selectively reflecting impinging waves [1]–[3]. As such, BF and RIS have synergistic roles, such that the optimization of BF weights and RIS parameters needs to be considered jointly.

In our prior work on this topic [4], [5] a novel method to design reciprocal BD-RIS (RBD-RIS) scattering matrices was proposed, whereby the challenging problem of maximizing the system’s sum-rate while incorporating a reciprocal structure that enforces both unitary and symmetry constraints was addressed under a manifold optimization framework. In accordance with state-of-the-art (SotA) approaches, the system model considered in the aforementioned work was a multi-user (MU)-multiple-input single-output (MISO) setup, which facilitates comparison, analysis, and highlights the gains obtained from the scattering matrix design. Nevertheless, the assumption of a single antenna user is restrictive, thereby motivating the extension to a generalized MU cell-free (CF)-massive multiple-input multiple-output (mMIMO) setup.

The proposed solution provides a structured approach applicable to various beyond diagonal reconfigurable intelligent surface (BD-RIS) architectures, namely single-, group-, and fully-connected, while also showing promising performance improvements compared to the SotA methods. Building upon the foundation established in [5], this article addresses the accompanying system optimization problem, namely, the beamforming matrix design. To elaborate further, while the scattering matrix determines how signals are manipulated at the RIS, the beamforming matrix specifies the active transmission strategy at the access points (APs) [6]–[8], such that the joint optimization of both is crucial to fully exploit the potential of BD-RIS structures.

In recognition of the above, considerable research has been done on the design of beamforming methods in combination with RISs [9]–[14]. Among such approaches, a widely adopted strategy for transmit (TX)-BF design is the use of fractional programming (FP) techniques, which effectively handle non-convex optimization problems and provide near-optimal solutions, making them well-suited to systems seeking high performance with manageable computational complexity. To cite an excellent example, Li *et al.* [9] formulated two beamforming design problems for BD-RIS with reflective and hybrid/multi-sector modes. In the first scenario, a point-to-point multiple-input multiple-output (MIMO) system aided

I. A. M. Sandoval, M. Fidanovski, H. S. Rou, G. T. F. de Abreu are with the School of Computer Science and Engineering, Constructor University (previously Jacobs University Bremen), Campus Ring 1, 28759 Bremen, Germany (emails: {imorales, mfidanovski, hrou, gabreu}@constructor.university).

E. Björnson is with the Department of Computer Science, KTH Royal Institute of Technology, Stockholm, Sweden (email: emilbjo@kth.se).

by a reflective mode BD-RIS was considered, where a joint optimization of the scattering and precoding matrices was developed and addressed using a two-stage approach. The proposed two-stage approach first designed the BD-RIS scattering matrix to maximize the effective channel strength, and then obtained the precoding matrix from the left unitary matrix following an singular value decomposition (SVD) of the resulting channel. In the second scenario, a MU-MISO system aided by a hybrid/multi-sector mode BD-RIS was considered, and a similar joint optimization problem was proposed. The problem was then reformulated using FP techniques, and transformed into a four-block optimization problem, where the blocks were iteratively updated until convergence. Namely, the precoding block solution was obtained based on the Karush-Kuhn-Tucker (KKT) conditions. A similar solution, based on the FP approach for the TX beamformer, was obtained in [10]. Both works are limited in that the scattering matrix design does not account for the reciprocal structure of the BD-RIS.

Beamforming designs for RISs have also been investigated in the context of integrated sensing and communications (ISAC) systems [11], [12]. For instance, in [11], a MU-MISO ISAC system aided by a fully-connected BD-RIS was considered, where a joint optimization problem was formulated for the design of the linear filter, beamforming and scattering matrices, aiming to maximize network throughput while satisfying radar sensing quality constraints. The problem was then addressed using FP techniques combined with the majorization-minimization method, transforming it into a convex form and enabling computation of the optimal TX beamformer. Additionally, in [12], a millimeter-wave (mmWave) ISAC system with a BD-RIS-aided transmitter was studied, where a joint design of digital beamforming, scattering, and digital radar covariance matrices was proposed to enhance both communication and sensing performance. Following a conventional two-stage approach, the scattering matrix was optimized first, followed by the TX beamformer. The corresponding TX beamforming matrix was obtained by formulating an optimization problem, introducing slack variables, and applying multiple successive convex approximation (SCA) iterations along with an eigenvalue decomposition (EVD) on the resulting suboptimal solution.

An alternative approach was proposed in [13], where a power minimization and energy efficiency maximization problem was formulated for a downlink MU-MISO network, each requiring the design of the corresponding TX beamformers. For power minimization, the AP beamformer is obtained via a second-order cone programming (SOCP) problem formulation, allowing for an optimal solution to be obtained using standard numerical solvers like CVX [15]. In turn, for the energy efficiency maximization problem, the AP-BF matrix was designed following conventional FP transformation methods. While effective, the approach relies on generic convex optimization solvers and entails relatively high computational complexity. To alleviate this issue, a related approach was presented in [16], where the beamforming matrix was optimized as a block variable using a partially proximal alternating direction method of multipliers (pp-ADMM) framework, enabling more efficient iterative updates.

Additionally, in [14] a RIS-aided MU-MISO system was considered and an optimization problem was formulated. Similarly to the approach in this article, FP techniques are applied to the objective function, followed by a Lagrange multiplier method, allowing for the optimal precoder to be obtained by verifying the first-order optimality conditions. The Lagrange multiplier was determined using a simple bisection search.

A common limitation of all the aforementioned methods¹ is, however, that the beamforming matrix is obtained without enforcing sub-array power constraints, such that the results cannot be used directly in distributed BF scenarios. To elaborate further, if not a single but a set of APs collaborate in a distributed BF fashion to transmit signals to users [19], under a condition where each AP is subjected to its own TXs power constraint [20]–[22], *e.g.*, due to particular hardware limitations or local regulatory restrictions [23], [24], [25], [26], the optimal collective BF matrix must have blocks with distinct powers. This constraint is difficult to enforce under conventional approaches where the entries of the BF matrix are optimized as free-complex numbers, that is, such that both the amplitude and the phase of antenna coefficients are allowed to take on any values.

In this context, [20] considered a downlink RIS-aided CF-mMIMO network, whereby a FP approach along with alternating optimization (AO) methods were utilized to obtain the hybrid BF matrix at the base station (BS) under per-AP power constraints. This work is however limited in that it only considers a conventional diagonal RIS structure. In a related direction, [22] proposed a decentralized BF framework for multi-BD-RIS-assisted CF-mMIMO Orthogonal Frequency Division Multiplexing (OFDM) systems, where the non-convex sum-rate maximization problem is addressed via successive convex approximation using first-order surrogate functions. In particular, that work considers a wideband setting with multiple shared BD-RISs and jointly optimizes the precoders together with the tunable capacitance and permutation matrices through consensus-based updates. Rather than designing the scattering matrix directly, the passive configuration is obtained through a circuit-based parametrization that guarantees reciprocity. This offers a valuable and practically motivated perspective on scalable multi-BD-RIS optimization.

In contrast to prior approaches, this article addresses the joint design of per-AP TX BF and multiple RBD-RIS scattering matrices using FP techniques, which transform the original non-convex problem into a sequence of tractable convex subproblems, enabling efficient optimization under practical constraints. To the best of our knowledge, this is the first work to consider the aforementioned FP-framework in a general CF-mMIMO setting. Overall, the main contributions of this article can be summarized as follows:

- A novel BF matrix design is proposed for RBD-RIS-aided MU CF-mMIMO systems, where the amplitude and phase coefficients of the antenna elements are optimized separately, offering flexibility that enables distributed (collaborative) BF.

¹This limitation applies also to alternative BF that are not based on the FP approach, *e.g.*, [17], [18].

- A generalized closed form expression for the gradient of the objective function with respect to the scattering matrix is provided, enabling its optimization using the algorithm proposed in [5] over multiple independent RBD-RIS.
- A closed form expression for the proposed FP-based sub-BF matrix is given, which allows for an optimal solution to be found using a simple two-dimensional (2D)-search, yielding overall a low-complexity alternative to BF for RBD-RIS-aided MU CF-mMIMO systems.

Organization: The remainder of the article is organized as follows. Section II introduces the BD-RIS-aided MU CF-mMIMO system model, presents the decomposition of the TX beamforming matrix, and formulates the problem considered in this article. Following the problem formulation, Section III provides a solution for the TX beamforming matrix design. Simulation results are provided in Section IV, which help evaluate the performance of the proposed designs. Conclusions and possible future work directions are discussed in Section V.

Notation: Unless otherwise specified, \mathbf{X} and \mathbf{x} denote matrices and vectors. The absolute value, ℓ^2 and Frobenius norm are denoted by $|\cdot|$, $\|\cdot\|_2$, $\|\cdot\|_F$. The transpose and the Hermitian transpose are denoted by $(\cdot)^T$ and $(\cdot)^H$. $\mathbf{X}_{i,j}$ denotes the i -th row and j -th column element of the matrix \mathbf{X} , $\mathbf{X}_{i:\bar{i},j:\bar{j}}$ extracts the elements from the i -th to the \bar{i} -th row, and j -th to \bar{j} column from the matrix \mathbf{X} , $\text{diag}(\mathbf{x}) = (x_1, x_2, \dots, x_k)$ denotes a diagonal matrix, where the main diagonal is \mathbf{x} , $\text{blkdiag}(\mathbf{X}_1, \mathbf{X}_2, \dots, \mathbf{X}_k)$ denotes a $G \times G$ block diagonal matrix with off diagonal elements 0, where the blocks are $\mathbf{X}_1, \mathbf{X}_2, \dots, \mathbf{X}_k$. The set of complex and real numbers is denoted by \mathbb{C} and \mathbb{R} , $\Re\{\cdot\}$ and $\Im\{\cdot\}$ denote the real and imaginary values of a complex number, respectively. $\mathcal{CN}(0, \sigma^2)$ denotes a complex normal random variable with a zero mean and σ^2 variance. Finally, $\log_n |\cdot|$ denotes the log determinant.

II. SYSTEM MODEL

A. System and Channel Model

Consider a downlink BD-RIS-aided MU CF-mMIMO system as illustrated in Figure 1, where L interconnected APs with N_a TX antennas each, resulting in a total number of $N_t = L \times N_a$ antennas, service K users with M receive (RX) antennas each, with the assistance of a BD-RIS consisting of R reflective elements (REs) located between the APs and users².

For convenience, let $\mathcal{L} \triangleq \{1, 2, \dots, L\}$ and $\mathcal{K} \triangleq \{1, 2, \dots, K\}$ be the sets of indices l and k , corresponding to APs and users, respectively. Furthermore, $\Theta \in \mathbb{C}^{R \times R}$ denotes the BD-RIS scattering matrix, the channel linking the l -th AP and the BD-RIS (i.e., the AP $_l$ -to-BD-RIS channel) is denoted as $\mathbf{H}_{\text{TX},l} \in \mathbb{C}^{R \times N_a}$, and the BD-RIS-to-user k channel matrix is given by $\mathbf{H}_{\text{RX},k} \in \mathbb{C}^{M \times R}$. The transmit signal vector is denoted as $\mathbf{x}_k = \mathbf{V}_k \mathbf{s}_k$, where the information symbols $\mathbf{s}_k \in \mathbb{C}^{M \times 1}$ corresponding to the k -th user satisfy $\mathbb{E}[\mathbf{s}_k \mathbf{s}_k^H] = \mathbf{I}$, and the TX beamforming matrix from all APs to U_k , i.e., $\mathbf{V}_k \in \mathbb{C}^{N_t \times M}$ meets the power constraint $\sum_{k \in \mathcal{K}} \|\mathbf{V}_k\|_F^2 \leq P_{\max}$, with P_{\max} being the maximum power that is available to the system.

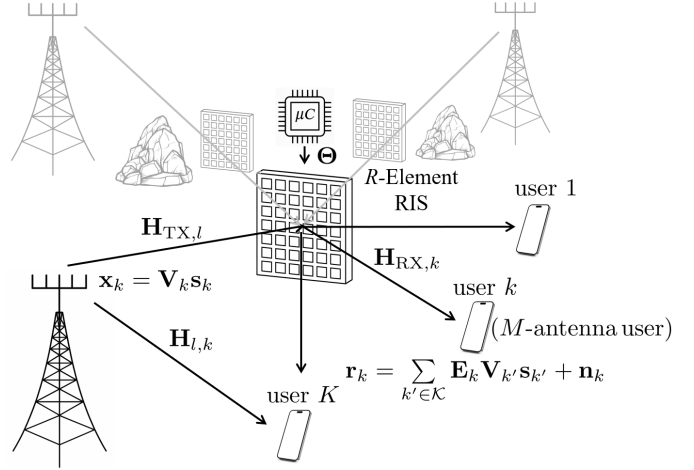


Figure 1: Illustration of the system model, where L APs with N_a TX antennas each serve K users with M RX antennas each through multiple R -element RBD-RISs with a direct line-of-sight (LoS) link between the APs and the users.³

The equivalent channel linking the l -th AP to the k -th user, including both the direct LoS and BD-RIS-aided path can be defined as $\mathbf{E}_{l,k} = \mathbf{H}_{l,k} + \mathbf{H}_{\text{RX},k} \Theta \mathbf{H}_{\text{TX},l}$, such that $\mathbf{E}_{l,k} \in \mathbb{C}^{M \times N_a}$.

Straightforwardly, the equivalent downlink channel matrix from all APs to U_k is obtained as the concatenation of the AP $_l$ - U_k equivalent channels, namely

$$\mathbf{E}_k \triangleq [\mathbf{E}_{1,k}, \mathbf{E}_{2,k}, \dots, \mathbf{E}_{L,k}] \in \mathbb{C}^{M \times N_t}. \quad (1)$$

Considering the channel model, the matrices $\mathbf{H}_{\text{TX},l}$, $\mathbf{H}_{\text{RX},k}$, and $\mathbf{H}_{l,k}$ are generated using a narrowband Rician fading model with distance-dependent large-scale fading.⁴ Specifically, each channel realization is expressed as

$$\mathbf{H} = \sqrt{\Upsilon(d)} \left(\sqrt{\frac{K_f}{K_f + 1}} \mathbf{H}_{\text{LoS}} + \sqrt{\frac{1}{K_f + 1}} \mathbf{H}_{\text{NLoS}} \right), \quad (2)$$

where $\Upsilon(d)$ denotes the large-scale fading coefficient and K_f is the Rician factor. The NLoS component \mathbf{H}_{NLoS} consists of independent and identically distributed complex Gaussian entries, whereas the LoS component is modeled using a geometric rank-one representation based on uniform linear arrays (ULAs), given by

$$\mathbf{H}_{\text{LoS}} = e^{-j \frac{2\pi d}{\lambda}} \mathbf{a}_{\text{rx}}(\theta_{\text{AoA}}) \mathbf{a}_{\text{tx}}^H(\theta_{\text{AoD}}), \quad (3)$$

where d is the link distance, λ is the carrier wavelength, and $\mathbf{a}_{\text{rx}}(\cdot)$ and $\mathbf{a}_{\text{tx}}(\cdot)$ denote the receive and transmit array response vectors, respectively. The angles of arrival and departure are independently drawn from $[-\pi/2, \pi/2]$.

Thus, the complex baseband received signal at the k -th user can be expressed as

$$\mathbf{r}_k = \overbrace{\mathbf{E}_k \mathbf{V}_k \mathbf{s}_k}^{\text{Intended signal}} + \overbrace{\sum_{k' \in \mathcal{K} \setminus \{k\}} \mathbf{E}_k \mathbf{V}_{k'} \mathbf{s}_{k'}}^{\text{Downlink inter-user interference}} + \mathbf{n}_k, \quad (4)$$

³This setting represents the most general scenario, aimed at highlighting the impact of the joint scattering and the BF matrix design.

⁴Details on the large-scale fading model are provided in Section IV, where different parameters are specified for the AP-to-BD-RIS, BD-RIS-to-user, and direct AP-to-user links.

²The extension to multiple BD-RIS is detailed in Appendix A.

where $\mathbf{r}_k \in \mathbb{C}^{M \times 1}$ and $\mathbf{n}_k \in \mathbb{C}^{M \times 1} \sim \mathcal{CN}(0, N_0 \mathbf{I})$ denotes the circularly symmetric additive white Gaussian noise (AWGN) noise at user k with the power spectral density N_0 .

B. Problem Formulation

From the received signal model, it follows that the interference-plus-noise-whitened signal covariance matrix received at the k -th user, $\mathbf{\Gamma}_k$, can be formulated as

$$\mathbf{\Gamma}_k = \mathbf{V}_k^H \mathbf{E}_k^H \mathbf{\Psi}_k^{-1} \mathbf{E}_k \mathbf{V}_k, \quad (5a)$$

where

$$\mathbf{\Psi}_k \triangleq \sum_{k' \in \mathcal{K} \setminus \{k\}} \mathbf{E}_k \mathbf{V}_{k'} \mathbf{V}_{k'}^H \mathbf{E}_k^H + N_0 \mathbf{I}_M, \quad (5b)$$

is the corresponding interference-plus-noise covariance matrix.

The TX beamformer for user k can be further divided into

$$\mathbf{V}_k \triangleq \begin{bmatrix} \mathbf{Q}_{1,k} \\ \mathbf{Q}_{2,k} \\ \vdots \\ \mathbf{Q}_{L,k} \end{bmatrix}, \forall k \in \mathcal{K}, \quad (6)$$

where $\mathbf{Q}_{l,k} \in \mathbb{C}^{N_a \times M}$ represents the sub-BF matrices from the l -th AP, to service user k , and can be collected into

$$\mathbf{Q}_l \triangleq [\mathbf{Q}_{l,1}, \mathbf{Q}_{l,2}, \dots, \mathbf{Q}_{l,K}], \forall l \in \mathcal{L}, \quad (7)$$

such that $\mathbf{Q}_l \in \mathbb{C}^{N_a \times (K \cdot M)}$ is the TX beamforming matrix local to the l -th AP.

Following the formulation in [5], the power-constrained sum-rate maximization problem is described as

$$(P1): \quad \underset{\mathbf{V}_k, \Theta}{\text{maximize}} \quad \sum_{k \in \mathcal{K}} \log_2 |\mathbf{I}_M + \mathbf{\Gamma}_k| \quad (8a)$$

$$\text{subject to} \quad \sum_{k \in \mathcal{K}} \|\mathbf{V}_k\|_{\mathbb{F}}^2 \leq P_{\max}, \quad (8b)$$

$$\|\mathbf{Q}_l\|_{\mathbb{F}}^2 \leq P_l, \forall l \in \mathcal{L}, \quad (8c)$$

$$\Theta \in \mathcal{S}_{a_1}, \quad (8d)$$

$$\Theta \in \mathcal{S}_{a_2}, \quad (8e)$$

where $a \in \{\text{SC}, \text{FC}, \text{GC}\}$ denotes the connectivity level of the BD-RIS, P_{AP} is the maximum transmit power available at each AP, such that $P_{\max} \triangleq \sum_{l \in \mathcal{L}} P_l$.

It is evident that the optimization problem described in (8) is inherently non-convex, due to both the objective function in (8a) and the constraints in (8b)-(8e). The scattering matrix is subject to degrees-of-freedom (DoF) restrictions imposed by the reciprocal and lossless properties of the BD-RIS, which are generally non-convex [5]. Additionally, the constraints on the beamforming and sub-BF matrix are non-convex. For simplicity, the sum-rate over all users is denoted as

$$\eta \triangleq \sum_k \eta_k, \quad \text{with} \quad \eta_k \triangleq \log_2 |\mathbf{I}_M + \mathbf{\Gamma}_k|. \quad (9)$$

While [5] focuses on the design of the scattering matrix for RBD-RIS under specific conditions that highlight its impact on the system sum-rate, this work generalizes that study by additionally considering the second stage, namely the design of the beamforming matrix.

III. STAGE 2: BEAMFORMING MATRIX DESIGN

Since a CF-mMIMO system is considered in this article, a generalization of the solution for the scattering matrix design proposed in [5] to the MIMO case is required. Straightforwardly, we mitigate the issue of non-convexity of the log-ratio term in the objective function (8a) by applying the matrix FP method described in [27]–[29].

To this extent, upon applying the Lagrangian Dual Transform (LDT) to η_k the following is obtained

$$\begin{aligned} \bar{\eta}_k &= \log_2 |\mathbf{I}_M + \mathbf{Z}_k| - \text{Tr}(\mathbf{Z}_k) \\ &+ \text{Tr} \left((\mathbf{I}_M + \mathbf{Z}_k) \mathbf{V}_k^H \mathbf{E}_k^H \mathbf{\Psi}_k^{-1} \mathbf{E}_k \mathbf{V}_k \right), \end{aligned} \quad (10)$$

where $\mathbf{\Psi}_k$ denotes the interference term at the k -th user defined in (5b), and the auxiliary variable (i.e., the matrix Lagrange multiplier \mathbf{Z}_k) is given by

$$\mathbf{Z}_k = \mathbf{V}_k^H \mathbf{E}_k^H \mathbf{\Psi}_k^{-1} \mathbf{E}_k \mathbf{V}_k. \quad (11)$$

Furthermore, the Quadratic Transform (QT) is applied due to the ratio on the variable \mathbf{V}_k embedded in the last term of $\bar{\eta}_k$ as follows

$$\begin{aligned} \check{\eta}_k &= \log_2 |\mathbf{I}_M + \mathbf{Z}_k| - \text{Tr}(\mathbf{Z}_k) \\ &+ \text{Tr} \left((\mathbf{I}_M + \mathbf{Z}_k) (2\Re\{\mathbf{V}_k^H \mathbf{E}_k^H \mathbf{Y}_k\} - \mathbf{Y}_k^H \mathbf{\Psi}_k \mathbf{Y}_k) \right), \end{aligned} \quad (12)$$

where the auxiliary variable corresponding to the QT, namely \mathbf{Y}_k is given by

$$\mathbf{Y}_k = (\mathbf{E}_k \mathbf{V}_k \mathbf{V}_k^H \mathbf{E}_k^H + \mathbf{\Psi}_k)^{-1} \mathbf{E}_k \mathbf{V}_k. \quad (13)$$

For brevity, the constant terms are omitted and $\check{\eta}_k$ is rewritten as seen in (14), located at the top of the next page.

To derive a general solution, the group-wise definition for the equivalent channel is considered, namely

$$\mathbf{E}_{l,k}^{(g)} = \mathbf{H}_{l,k} + \mathbf{H}_{\text{RX},k}^{(g)} \Theta_g \mathbf{H}_{\text{TX},l}^{(g)}, \quad (15)$$

where $\mathbf{H}_{\text{RX},k}^{(g)} = \mathbf{H}_{\text{RX},k[1:M, R_G(g-1)+1: gR_G]}$, s.t. $\mathbf{H}_{\text{RX},k}^{(g)} \in \mathbb{C}^{M \times R_G}$, $\Theta_g = \Theta_{[R_G(g-1)+1: gR_G, R_G(g-1)+1: gR_G]}$, s.t. $\Theta_g \in \mathbb{C}^{R_G \times R_G}$, $\mathbf{H}_{\text{TX},l}^{(g)} = \mathbf{H}_{\text{TX},l[R_G(g-1)+1: gR_G, 1:N_a]}$, s.t. $\mathbf{H}_{\text{TX},l}^{(g)} \in \mathbb{C}^{R_G \times N_a}$, and $\mathbf{E}_{l,k}^{(g)} \in \mathbb{C}^{M \times N_a}$, where $g \in \{1, 2, \dots, G\}$ denotes the group, and R_G the group size. The group-wise equivalent downlink channel matrix from all APs to the k -th user is obtained following the method described in equation (1). As such, to obtain a solution for the BD-RIS scattering matrix design, the gradient of the objective function with respect to Θ_g is required.

For convenience, the corresponding gradient is derived as a closed-form expression, given in (17), seen at the top of the next page. For clarity, the concatenated equivalent channel in (1) can be rewritten as

$$\mathbf{E}_k = \bar{\mathbf{H}}_k + \mathbf{H}_{\text{RX},k} \Theta \bar{\mathbf{H}}_{\text{TX}}, \quad (16)$$

where the LoS channel matrix from all APs to the k -th user is denoted as $\bar{\mathbf{H}}_k = [\mathbf{H}_{1,k}, \mathbf{H}_{2,k}, \dots, \mathbf{H}_{L,k}] \in \mathbb{C}^{M \times N_t}$, and the aggregated AP-to-BD-RIS channel is given by $\bar{\mathbf{H}}_{\text{TX}} = [\mathbf{H}_{\text{TX},1}, \mathbf{H}_{\text{TX},2}, \dots, \mathbf{H}_{\text{TX},L}] \in \mathbb{C}^{R \times N_t}$.

$$\begin{aligned}\check{\eta}_k &= \text{Tr}\left((\mathbf{I}_M + \mathbf{Z}_k)(2\Re\{\mathbf{V}_k^H \mathbf{E}_k^H \mathbf{Y}_k\} - \sum_{k' \in \mathcal{K}} \mathbf{Y}_k^H \mathbf{E}_k \mathbf{V}_{k'} \mathbf{V}_{k'}^H \mathbf{E}_k^H \mathbf{Y}_k)\right) \\ &= 2 \cdot \text{Tr}\left((\mathbf{I}_M + \mathbf{Z}_k)\Re\{\mathbf{V}_k^H \mathbf{E}_k^H \mathbf{Y}_k\}\right) - \text{Tr}\left(\sum_{k' \in \mathcal{K}} (\mathbf{I}_M + \mathbf{Z}_k) \mathbf{Y}_k^H \mathbf{E}_k \mathbf{V}_{k'} \mathbf{V}_{k'}^H \mathbf{E}_k^H \mathbf{Y}_k\right)\end{aligned}\quad (14)$$

$$\nabla_{\boldsymbol{\theta}_g} \check{\eta} = \sum_{k \in \mathcal{K}} \left[\mathbf{H}_{\text{RX},k}^{(g)H} \mathbf{Y}_k (\mathbf{I}_M + \mathbf{Z}_k) \mathbf{V}_k^H \bar{\mathbf{H}}_{\text{TX}}^{(g)H} - \mathbf{H}_{\text{RX},k}^{(g)H} \mathbf{Y}_k (\mathbf{I}_M + \mathbf{Z}_k) \mathbf{Y}_k^H \mathbf{E}_k \left(\sum_{k' \in \mathcal{K}} \mathbf{V}_{k'} \mathbf{V}_{k'}^H \right) \bar{\mathbf{H}}_{\text{TX}}^{(g)H} \right] \quad (17)$$

As a result of having obtained the scattering matrix, the beamforming matrix \mathbf{V}_k depends only on the effective channel \mathbf{E}_k . Therefore, (P1) can be rewritten as

$$(P2): \quad \underset{\mathbf{V}_k}{\text{maximize}} \quad \sum_{k \in \mathcal{K}} \check{\eta}_k \quad (18a)$$

$$\text{subject to} \quad \sum_{k \in \mathcal{K}} \|\mathbf{V}_k\|_F^2 \leq P_{\max}, \quad (18b)$$

$$\|\mathbf{Q}_l\|_F^2 \leq P_l, \quad \forall l \in \mathcal{L}. \quad (18c)$$

Furthermore, the problem can be expressed solely in terms of $\mathbf{Q}_{l,k}$ sub-beamformers as

$$(P3): \quad \underset{\mathbf{Q}_{l,k}}{\text{maximize}} \quad \sum_{k \in \mathcal{K}} \check{\eta}_k \quad (19a)$$

$$\text{subject to} \quad \sum_{k \in \mathcal{K}} \|\mathbf{Q}_{l,k}\|_F^2 \leq P_l, \quad \forall l \in \mathcal{L}. \quad (19b)$$

Based on the previous problem, the allocation of power to each AP based on the global available power and the power-beamforming direction breakdown, a FP successive convex optimization (SCO) can be written as

$$(P4): \quad \underset{\mathbf{Q}_{l,k}, p_{l,k}, \nu_l}{\text{maximize}} \quad \sum_{k \in \mathcal{K}} \check{\eta}_k \quad (20a)$$

$$\text{subject to} \quad \|\bar{\mathbf{Q}}_{l,k}\|_F^2 = 1, \quad \forall l, k \in \mathcal{L}, \mathcal{K}, \quad (20b)$$

$$\sum_{k \in \mathcal{K}} p_{l,k} \leq P_l, \quad \forall l \in \mathcal{L}, \quad (20c)$$

where

$$\mathbf{Q}_{l,k} = \sqrt{p_{l,k}} \bar{\mathbf{Q}}_{l,k}. \quad (21)$$

Finally, $\check{\eta}_k$, as seen in (14), can be set as

$$\check{\eta}_k = 2 \cdot \text{Tr}\left(\Re\{\mathbf{V}_k^H \mathbf{A}_k\}\right) - \text{Tr}\left(\sum_{k' \in \mathcal{K}} \mathbf{V}_{k'} \mathbf{V}_{k'}^H \mathbf{B}_k\right), \quad (22)$$

where for convenience, equivalent matrices \mathbf{A}_k and \mathbf{B}_k under the rotational property of the trace have been introduced as

$$\mathbf{A}_k = \mathbf{E}_k^H \mathbf{Y}_k (\mathbf{I}_M + \mathbf{Z}_k), \quad (23)$$

$$\mathbf{B}_k = \mathbf{E}_k^H \mathbf{Y}_k (\mathbf{I}_M + \mathbf{Z}_k) \mathbf{Y}_k^H \mathbf{E}_k. \quad (24)$$

Under the definition of (6), the two trace terms can be rewritten as

$$\begin{aligned}\check{\eta}_k &= 2 \sum_{l \in \mathcal{L}} \text{Tr}\left(\Re\{\mathbf{Q}_{l,k}^H [\mathbf{A}_k]_l\}\right) \\ &\quad - \sum_{k' \in \mathcal{K}} \sum_{l \in \mathcal{L}} \sum_{l' \in \mathcal{L}} \text{Tr}\left(\mathbf{Q}_{l,k'} \mathbf{Q}_{l',k'}^H [\mathbf{B}_k]_{l',l}\right),\end{aligned}\quad (25)$$

where $[\cdot]_l$ selects the l -th row group consisting of N_a rows, and $[\cdot]_{l',l}$ selects the l', l -th submatrix of size $N_a \times N_a$.

As such, the sum rate can be expressed as

$$\begin{aligned}\sum_{k' \in \mathcal{K}} \check{\eta}_{k'} &= 2 \sum_{k' \in \mathcal{K}} \sum_{l' \in \mathcal{L}} \text{Tr}\left(\Re\{\mathbf{Q}_{l',k'}^H [\mathbf{A}_{k'}]_{l'}\}\right) \\ &\quad - \sum_{k' \in \mathcal{K}} \sum_{k'' \in \mathcal{K}} \sum_{l' \in \mathcal{L}} \sum_{l'' \in \mathcal{L}} \text{Tr}\left(\mathbf{Q}_{l',k'} \mathbf{Q}_{l'',k''}^H [\mathbf{B}_{k'}]_{l',l''}\right).\end{aligned}\quad (26)$$

The first step towards the closed-form FP solution is to derive the sum rate with respect to $\mathbf{Q}_{l,k}$, as shown at the top of the next page of the article in (27).

Following the power constraints used in [30], the closed form can be obtained as

$$\mathbf{Q}_{l,k} = \left(\zeta_l \mathbf{I}_{N_a} + \sum_{k' \in \mathcal{K}} [\mathbf{B}_{k'}]_{l,l} \right)^{-1} \left([\mathbf{A}_k]_l - \frac{1}{2} \boldsymbol{\Omega}_{l,k} \right), \quad (28)$$

with

$$\boldsymbol{\Omega}_{l,k} = \sum_{k' \in \mathcal{K}} \sum_{l' \in \mathcal{L} \setminus \{l\}} \left([\mathbf{B}_{k'}]_{l,l'} + [\mathbf{B}_{k'}]_{l',l}^H \right) \underbrace{\mathbf{Q}_{l',k'}}_{\substack{\text{Treated as constant, updated} \\ \text{with minorizing matrices}}}. \quad (29)$$

For the convenience of the reader, the full procedure implemented in this article is outlined in Algorithm 1, and a convergence plot is provided in Figure 2, where it can be observed that the proposed BF algorithm converges rapidly, requiring ~ 10 iterations for all considered BD-RIS architectures, while higher-connectivity configurations achieve larger final sum-rate values without affecting the convergence speed.

Algorithm 1 Proposed FP-based per-AP BF Optimization

Input: \mathbf{E} , P_{\max} , N_0 , i_{\max}^{FP} , ζ_{\min} , ζ_{\max} , ϵ

Output: TX-beamforming matrix \mathbf{V}

Initialize: MMSE-based $\mathbf{V}^{(0)}$, $\mathbf{Q}_{l,k}^{(0)} \forall l, k$ from $\mathbf{V}_k^{(0)} \forall k$, $i^{\text{FP}} \leftarrow 0$

- 1: **repeat**
 - 2: $i^{\text{FP}} \leftarrow i^{\text{FP}} + 1$
 - 3: Compute $\mathbf{Z}_k, \forall k$ from (11)
 - 4: Compute $\mathbf{Y}_k, \forall k$ from (13)
 - 5: Compute $\mathbf{A}_k, \forall k$ from (23)
 - 6: Compute $\mathbf{B}_k, \forall k$ from (24)
 - 7: Obtain $\boldsymbol{\Omega}_{l,k}, \forall l, k$, following (29)
 - 8: Obtain $\mathbf{Q}_{l,k}^{(i^{\text{FP}})}, \forall l, k$, with optimized ζ_l via bisection search over $[\zeta_{\min}, \zeta_{\max}]$ to satisfy (8c)
 - 9: Compute $\mathbf{V}_k, \forall k$ from (6)
 - 10: **until** $\|\mathbf{V}^{(i^{\text{FP}})} - \mathbf{V}^{(i^{\text{FP}}-1)}\|_F < \epsilon, \forall k$ **or** $i^{\text{FP}} = i_{\max}^{\text{FP}}$
 - 11: **return** \mathbf{V}
-

$$\frac{\partial}{\partial \mathbf{Q}_{l,k}} \sum_{k' \in \mathcal{K}} \check{\eta}_{k'} = 2([\mathbf{A}_k]_l)^H - 2\mathbf{Q}_{l,k}^H \sum_{k' \in \mathcal{K}} [\mathbf{B}_{k'}]_{l,l} - \sum_{k' \in \mathcal{K}} \sum_{l' \in \mathcal{L} \setminus \{l\}} \left(([\mathbf{B}_{k'}]_{l,l'}) \mathbf{Q}_{l',k} \right)^H + \mathbf{Q}_{l',k}^H [\mathbf{B}_{k'}]_{l',l} \quad (27)$$

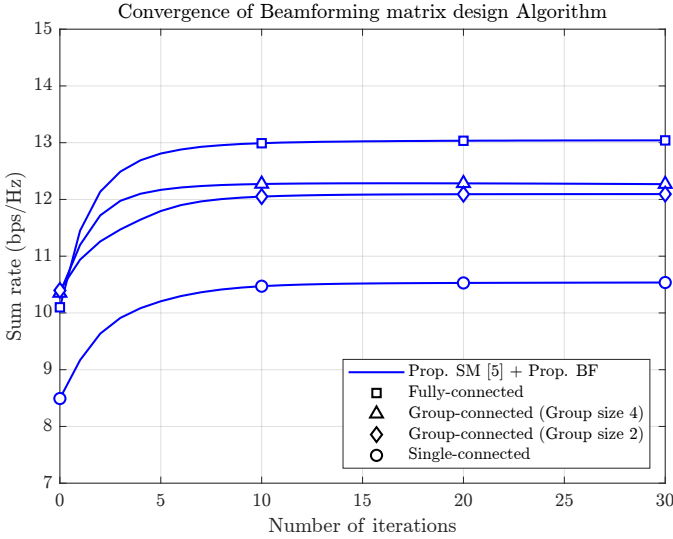


Figure 2: Convergence of Algorithm 1 vs. number of iterations for different connectivity structures, where $R = 32$, $M = 2$, $K = 4$, $N_a = 2$, $L = 4$ and $P_{\max} = 16$ dBm.

Computational Complexity: For the sake of comparison against existing SotA methods, a full computational complexity review is performed. The computational complexity of Algorithm 1 is mainly influenced by the number of bisection-search and FP iterations, i.e., i^{BS} and i^{FP} , in combination with computation of the sub-BF matrices. As such, for the computation of $\mathbf{Q}_{l,k} \forall l, k$, two loops over the L APs and K users are required, yielding a complexity of $\mathcal{O}(KL)$. Furthermore, in the worst case scenario, the inverse of the $N_a \times N_a$ matrix, yields a complexity of $\mathcal{O}(N_a^3)$. The inverse is then followed by an $N_a \times M$ matrix multiplication, which yields a total complexity for the computation of all sub-BF matrices equal to

$$\mathcal{O}(i^{\text{FP}} i^{\text{BS}} K L N_a^2 (N_a + M)). \quad (30)$$

Another source of considerable impact would be the computation of $\mathbf{\Omega}_{l,k}$, where four loops are considered to compute the full $\mathbf{\Omega}$ matrix, namely two loops going to K , one going to L and another going to $L - 1$, resulting in a complexity of $\mathcal{O}(K^2 L^2)$. The computation of $\mathbf{\Omega}$, further includes a multiplication of two matrices of size $N_a \times N_a$ and $N_a \times M$, yielding a total complexity of $\mathcal{O}(K^2 L^2 N_a^2 M)$. Taking account of all of the contributions, yields a total computational complexity of Algorithm 1 of

$$\mathcal{O}(i^{\text{FP}} (i^{\text{BS}} K L N_a^2 (N_a + M) + K^2 L^2 N_a^2 M)). \quad (31)$$

IV. SIMULATION RESULTS

This section evaluates the effectiveness of the proposed BF matrix design in improving the communication performance of RBD-RIS-aided CF-multiple-input multi-antenna

user multiple-output (MIMO) systems through computer simulations conducted under the following parameters.⁵

The number of users and APs depends on the considered scenario. Specifically, the performance of fully-, over-, and under-loaded systems is examined. The RIS structure consists of $R = 32$ REs, unless otherwise stated, and the parameters used for the scattering matrix design are identical to those in [5]; furthermore, each AP is subject to a maximum transmit power $P_{\text{AP}} = P_{\max}/L$, such that the total transmit power available to the system, P_{\max} , ranges from 0 to 16 dBm. The large-scale fading coefficients $\Upsilon(d)$ are generated using the 3rd Generation Partnership Project (3GPP) Urban Micro (UMi) path-loss models described in [31, Table B.1.2.1-1]. Specifically, the AP-to-BD-RIS and BD-RIS-to-user links are modeled as favorable LoS links, while the direct AP-to-user link is modeled as a strongly attenuated non-LoS (NLoS) link⁶. The small-scale fading is modeled as Rician fading for the LoS AP-to-BD-RIS and BD-RIS-to-user links, with Rician factor $K_f = 9$ dB, while the direct AP-to-user link is modeled as Rayleigh fading, corresponding to $K_f = 0$, in accordance with [31, Table B.1.2.2.1-4].

The link distances are set as $d = 2.5$ m for the BD-RIS-to-user link, $d = 50$ m for the AP-to-BD-RIS link, and $d = 51$ m for the AP-to-user link. The system operates at a carrier frequency of 2.4 GHz, and each user experiences identical noise with power spectral density $N_0 = -80$ dBm.

The first set of results is provided in Figure 3, and aims to demonstrate the effectiveness of the proposed BF matrix design against SotA methods [30], [32]. The scattering matrix “SM” follows the design proposed in [5], while the SotA BF schemes considered are the FP BF matrix from [30], and the minimum mean square error (MMSE) BF with per-AP power normalization [32]. The proposed BF design demonstrates clear performance improvements compared to both SotA methods at a transmit power of $P_{\max} = 16$ dBm. In particular, the combination of the proposed BF with the single-connected “SC” scattering matrix achieves notable sum-rate gains.

The second set of results, namely Figure 4, complements Figure 3 by illustrating the per-user rate performance of the proposed BF matrix design in combination with the scattering matrix “SM” design from [5], considering the single-connected architecture. The proposed method achieves superior per-user rates over most of the distribution, with only marginal degradation in a limited region. These gains mainly result from enforcing the per-AP power constraints within the sum-rate maximization. Despite this, the average performance remains consistently higher than that of the considered SotA methods.

⁵In all figures, except Figure 7, the scattering matrix is designed only following the approach in [5]. Since this work extends the aforementioned method, a direct extension of the comparisons presented therein is also provided.

⁶This configuration highlights the role of the BD-RIS in enhancing the propagation environment and is thus of practical relevance.

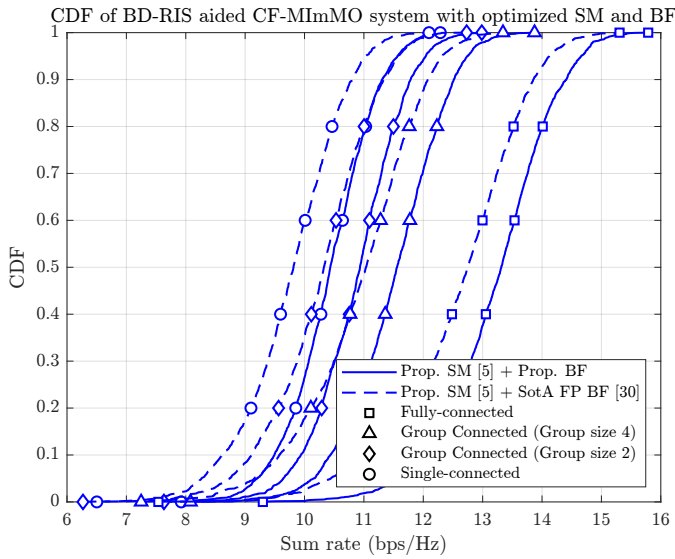


Figure 3: CDF of sum-rate performance of the proposed vs. SotA BF matrix design [30] with the fully-connected “FC”, group-connected “GC”, with group size of 2 and 4, and the single-connected “SC” architecture, where $R = 32$, $M = 2$, $K = 4$, $N_a = 2$, $L = 4$, $\nu = 1$, and $P_{\max} = 16$ dBm.

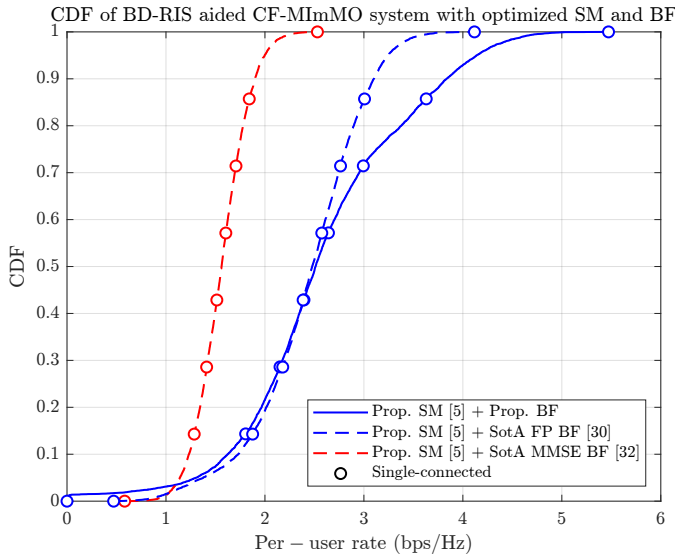
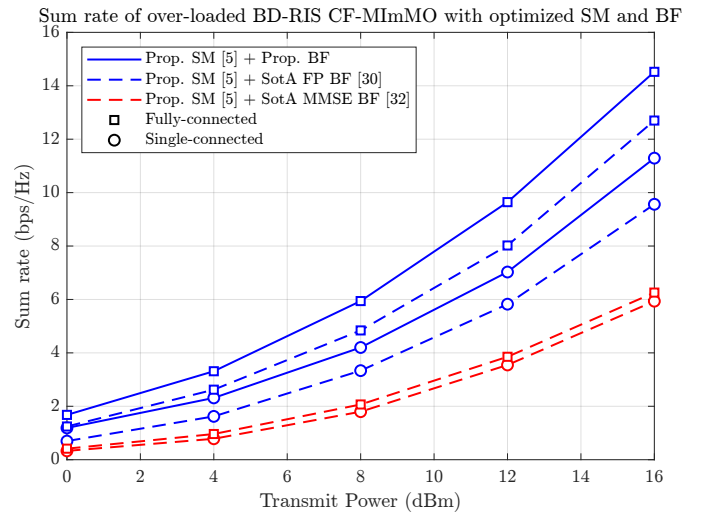


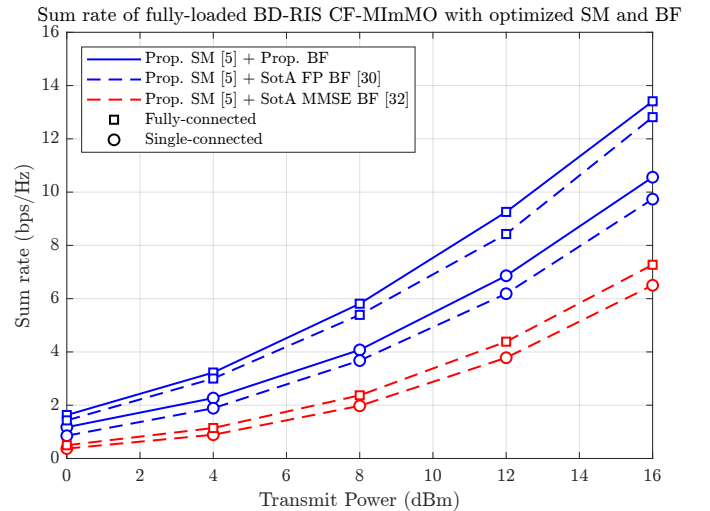
Figure 4: CDF of per-user rate performance of the proposed vs. SotA BF matrix designs [30], [32], considering the single-connected “SC” architecture, where $R = 32$, $M = 2$, $K = 4$, $N_a = 2$, $L = 4$, $\nu = 1$, and $P_{\max} = 16$ dBm.

Further assessments aim to demonstrate the performance of the proposed BF matrix design in combination with the proposed scattering matrix “SM” over a transmit power P_{\max} range, i.e., 0 – 16 dBm, under different loaded cases, namely over-, fully-, and under-loaded scenarios, respectively.

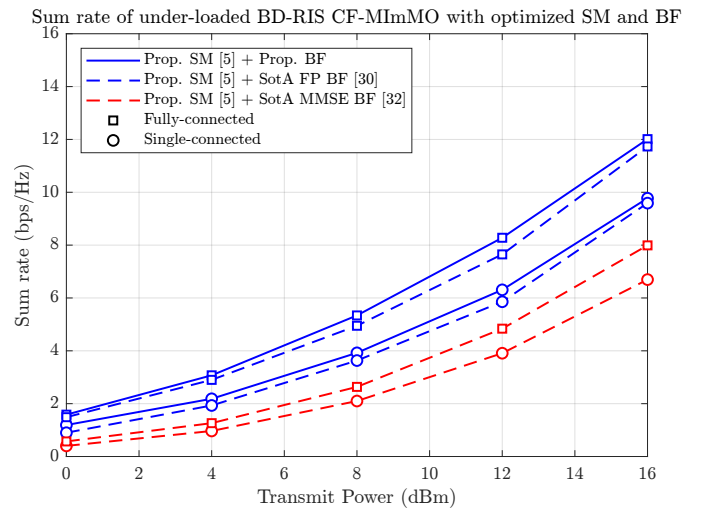
Namely, in Figure 5 the sum rate performance of the proposed BF matrix design in combination with the single-connected “SC” and fully-connected “FC” scattering matrix [5] is showcased. Complementary, Figure 6 assesses the sum-rate performance of the proposed BF matrix design in combination with the group-connected scattering matrix, with group size 2 and 4, “GC(2)” and “GC(4)”, respectively.



(a) Over-loaded ($K = 6$)



(b) Fully-loaded ($K = 4$)



(c) Under-loaded ($K = 3$)

Figure 5: Comparison of the sum-rate performance between the proposed method and the SotA BF matrix designs [30], [32] with the fully-, and single-connected, “FC” and “SC” architecture, under over-, fully-, and under-loaded system scenarios, where $R = 32$, $M = 2$, $N_a = 2$, $L = 4$, $\nu = 1$.

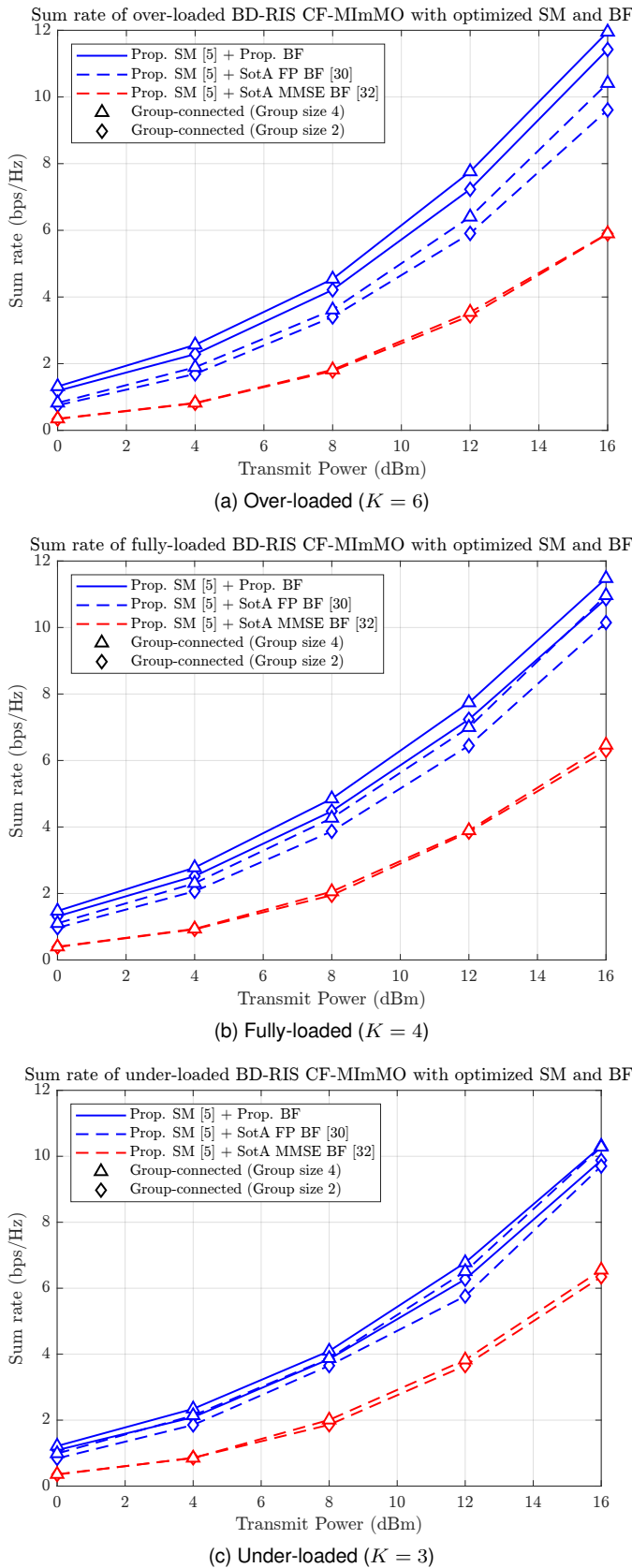


Figure 6: Comparison of the sum-rate performance between the proposed method and the SotA BF matrix designs [30], [32] with the group-connected ‘‘GC’’ architecture, with a group size 2 and 4, under over-, fully-, and under-loaded system scenarios, where $R = 32$, $M = 2$, $N_a = 2$, $L = 4$, $\nu = 1$.

The proposed BF matrix design exhibits consistent performance gains across different system loading regimes, including over-, fully-, and under-loaded scenarios, compared to the considered SotA methods. The most pronounced gains, together with the highest overall sum-rate values, are observed in the overloaded regime. In this case, the larger number of served users makes the system more interference-limited, which increases the importance of coordinating the distributed transmit resources under the per-AP power constraints. The proposed design performs this coordination more effectively than the considered SotA methods, leading to improved inter-user interference mitigation and higher performance. Nevertheless, the performance differences among the under-, fully-, and over-loaded cases remain relatively small. This indicates that, when many users are present, comparable average performance can be achieved by serving only a subset of users at a time, for example, through round-robin scheduling. Such an approach can reduce the system complexity while maintaining nearly the same performance level, since the overall sum-rate is not strongly affected by the considered loading regime.

As previously mentioned, the work done in this article constitutes an extension of [5], through the design of the BF matrix for the proposed scattering matrix design. For consistency, the same channel model as in [5] is adopted in the subsequent numerical evaluations, where the direct AP-to-user link is omitted. Therefore, the following figures present results that directly extend the comparisons reported in [5] by incorporating the proposed BF matrix design into the comparisons presented in that article.

As such, Figure 7 presents a comparison of the sum-rate performance of the proposed scattering matrix ‘‘SM’’ [5], in combination with either uniform power allocation ‘‘PA’’, or the proposed BF, against the joint scattering and beamforming matrix design based on the pp-ADMM framework⁷ [16]. While the proposed BF design combined with the single-connected ‘‘SC’’ architecture exhibits a performance loss relative to the pp-ADMM method, the additional architectures considered, namely the group-connected ‘‘GC’’ architecture with group size 4 and the fully-connected ‘‘FC’’ architecture, achieve similar or slightly better performance, with similar computational complexity.⁸ Moreover, the considered system model, i.e., the CF-MIMO setting, together with the more general BF design, which is not restricted to the MU-MISO case, provides greater flexibility and broader applicability of the proposed framework. In addition, the reported results include scenarios with a larger number of RX antennas, M , thereby illustrating the behavior of the proposed approach in a more general MIMO setting.

⁷It should be noted that the aforementioned framework was originally developed for the MU-MISO scenario and therefore requires additional modifications to be applicable in the CF-MIMO setting. In contrast, the proposed framework can directly accommodate the less distributed MU-MISO case through appropriate selection of the system parameters.

⁸As shown in [5], the scattering matrix ‘‘SM’’ design, when combined with SotA BF methods, has a computational complexity comparable to that of the pp-ADMM framework. In the present work, however, we build upon the framework developed in [5], which introduces an additional additive term in the complexity, as given in (31). Under the sparse system setting considered in this comparison, this term is negligible relative to the computational complexity of the SM design in [5].

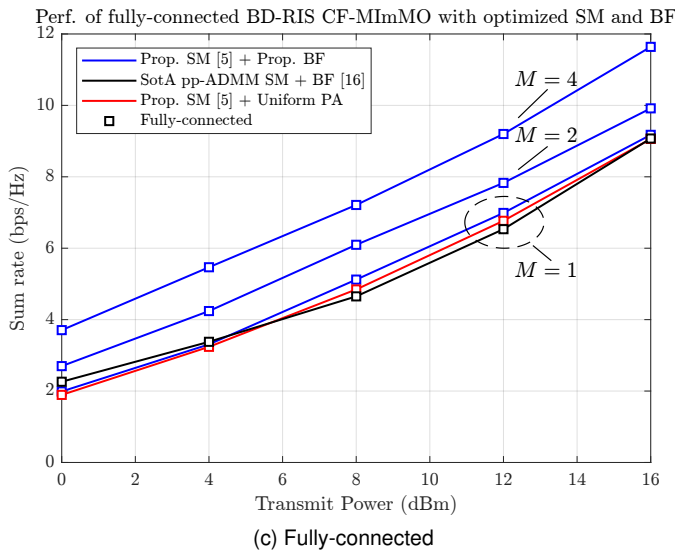
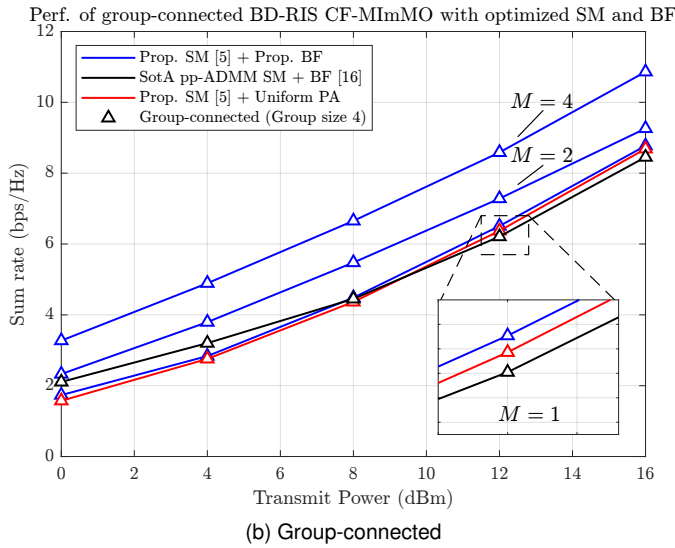
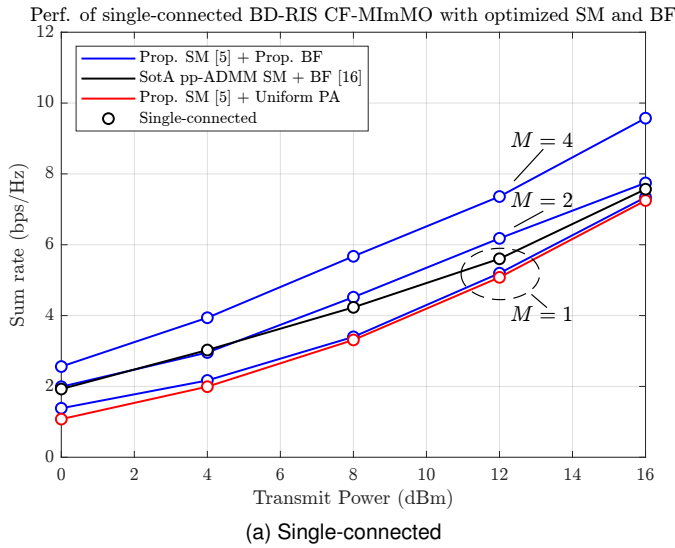


Figure 7: Comparison of the sum-rate performance using joint scattering matrix “SM” and “BF” schemes, considering the proposed and SotA [16] fully-connected “FC”, group-connected “GC” architecture, with a group size 4, and single-connected “SC” architecture, where $R = 32$, $M \in \{1, 2, 4\}$, $K = 2$, $N_a = 2$, $L = 1$, and $\nu = 1$.

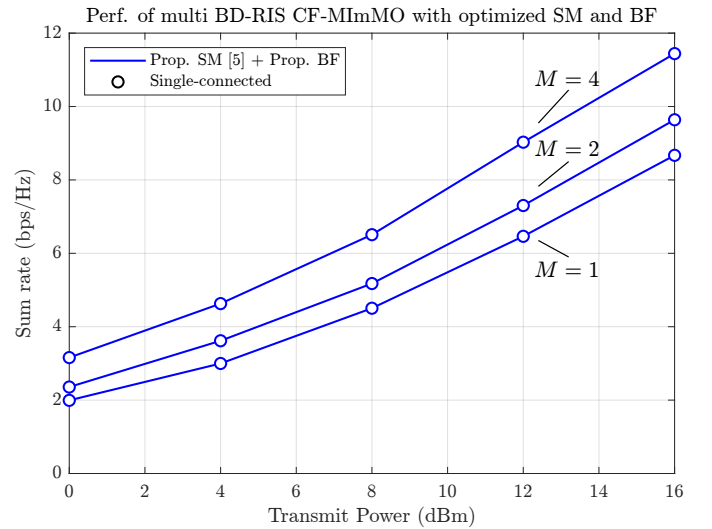


Figure 8: Sum-rate performance of the proposed BF matrix design in a setting with B deployed BD-RISs, considering the single-connected “SC” architecture, where $R = 16$, $B = 2$, $M \in \{1, 2, 4\}$, $K = 2$, $N_a = 2$, $L = 1$, and $\nu = 1$.

Lastly, in Figure 8, we present the sum-rate performance of the proposed BF matrix design in a scenario with multiple, B , BD-RISs.⁹ The simulation parameters for the multi-BD-RIS case are selected such that the deployed surfaces remain of comparable large-scale strength, either by retaining the baseline distances of the single BD-RIS setup or by introducing only mild asymmetry. This choice is made to highlight the gains enabled by the additional spatial flexibility of multiple deployed BD-RISs, rather than a regime in which one surface becomes effectively dominant. The results show that the proposed design can effectively exploit the additional DoFs offered by multiple deployed BD-RISs to further improve system performance. The results show that the proposed design can effectively exploit the additional DoFs offered by multiple deployed BD-RISs to further improve system performance. More specifically, for the same system parameters as in Figure 7, but with one additional BD-RIS and under the single-connected “SC” architecture, the achieved sum-rate becomes comparable to that attained by the fully-connected “FC” architecture. In particular, the combination of two smaller single-connected BD-RISs, each comprising 16 REs, is able to deliver similar performance to that of a single fully-connected BD-RIS with 32 REs. This highlights that distributing the available REs across multiple simpler surfaces can provide substantial performance gains, while avoiding the increased architectural complexity associated with a single larger fully-connected BD-RIS.

⁹It should be noted that, although [22] considers a related multi-BD-RIS CF-mMIMO setting, the system model and optimization framework differ materially from those considered herein. In particular, [22] studies a decentralized wideband OFDM design in which channel state information (CSI) is locally acquired and exchanged among the BSs, while the final BD-RIS configurations are obtained through consensus-based updates. By contrast, our work adopts a centralized design framework and focuses on FP-based per-AP beamforming together with direct scattering matrix optimization. Therefore, including [22] as a numerical benchmark would not constitute a direct and fair comparison.

It is further noted that the proposed framework is sufficiently general to accommodate heterogeneous multi-BD-RIS deployments, such that different surfaces may adopt different architectures, including single-connected, group-connected, and fully-connected configurations. Nevertheless, in this work, two single-connected BD-RISs are considered to facilitate a direct comparison with the previously presented results.

V. CONCLUSION

A novel sum-rate maximization BF matrix design scheme for RBD-RIS-aided CF-MIMO systems has been presented in this article. The proposed design is based on the FP framework and is developed to satisfy per-AP power constraints, while remaining applicable to a wide range of scattering matrix designs. In addition, the scattering matrix design method proposed in prior work has been extended to the more general MIMO setting, and a closed-form gradient expression has been derived, enabling efficient optimization via Riemannian manifold-based methods. Simulation results demonstrate the effectiveness of the proposed approach in improving the communication performance of RBD-RIS-aided CF-MIMO systems compared to SotA methods, across different system loading regimes, including over-, fully-, and under-loaded scenarios.

The results further highlight that the proposed design achieves consistent performance gains at both the system and user levels, while effectively handling the distributed nature of the network. In particular, the observed improvements in interference-limited regimes underline the importance of jointly optimizing the beamforming and scattering matrix under practical power constraints. Moreover, the results suggest that exploiting the additional spatial flexibility offered by multiple less complex BD-RISs may be more effective than increasing the architectural complexity of a single large BD-RIS. Overall, these findings confirm that the proposed framework provides a flexible and efficient solution for enhancing the performance of RBD-RIS-aided systems.

APPENDIX A

EXTENSION TO MULTIPLE BD-RISs

The system model in Section II can be extended to the case of multiple deployed BD-RISs by introducing a set of surfaces indexed by $b \in \{1, 2, \dots, B\}$, where each b -th BD-RIS is characterized by its scattering matrix $\Theta^{(b)} \in \mathbb{C}^{R_b \times R_b}$, the channel $\mathbf{H}_{\text{TX},l}^{(b)} \in \mathbb{C}^{R_b \times N_a}$ from the l -th AP to the b -th BD-RIS, and the channel $\mathbf{H}_{\text{RX},k}^{(b)} \in \mathbb{C}^{M \times R_b}$ from the b -th BD-RIS to the k -th user. Then, the equivalent channel between the l -th AP and the k -th user, which in the single-BD-RIS case is given by $\mathbf{E}_{l,k} = \mathbf{H}_{l,k} + \mathbf{H}_{\text{RX},k} \Theta \mathbf{H}_{\text{TX},l}$, is generalized as

$$\mathbf{E}_{l,k} = \mathbf{H}_{l,k} + \sum_{b=1}^B \mathbf{H}_{\text{RX},k}^{(b)} \Theta^{(b)} \mathbf{H}_{\text{TX},l}^{(b)}. \quad (32)$$

Accordingly, the aggregate downlink channel from all APs to user k becomes $\mathbf{E}_k = [\mathbf{E}_{1,k}, \mathbf{E}_{2,k}, \dots, \mathbf{E}_{L,k}]$, while the received signal model, the interference-plus-noise-whitened signal covariance matrix, and the subsequent FP-based beamforming design remain unchanged in form after replacing the

single-surface equivalent channel by the above multi-BD-RIS expression. In this case, the optimization variables are extended from Θ to the set $\{\Theta^{(b)}\}_{b=1}^B$, with each scattering matrix satisfying its corresponding reciprocity, losslessness, and connectivity constraints. This extension therefore preserves the overall structure of the proposed framework, while allowing the joint modeling of multiple BD-RIS-assisted propagation paths.

Approximate decoupling of the multi-BD-RIS contributions in the MIMO case: Let the effective channel of user k be extended from the single-BD-RIS model in (16) to

$$\mathbf{E}_k = \bar{\mathbf{H}}_k + \sum_{b=1}^B \mathbf{H}_{\text{RX},k}^{(b)} \Theta^{(b)} \bar{\mathbf{H}}_{\text{TX}}^{(b)}, \quad (33)$$

where, for convenience, we define

$$\mathbf{E}_k^{(0)} \triangleq \bar{\mathbf{H}}_k, \quad \mathbf{E}_k^{(b)} \triangleq \mathbf{H}_{\text{RX},k}^{(b)} \Theta^{(b)} \bar{\mathbf{H}}_{\text{TX}}^{(b)}, \quad b = 1, \dots, B, \quad (34)$$

such that

$$\mathbf{E}_k = \sum_{b=0}^B \mathbf{E}_k^{(b)}. \quad (35)$$

The corresponding rate at the k -th user is

$$\eta_k = \log_2 |\mathbf{I}_M + \mathbf{\Gamma}_k|, \quad \text{with } \mathbf{\Gamma}_k = \mathbf{V}_k^H \mathbf{E}_k \mathbf{\Psi}_k^{-1} \mathbf{E}_k \mathbf{V}_k \quad (36)$$

and

$$\mathbf{\Psi}_k = \sum_{i \neq k} \mathbf{E}_i \mathbf{V}_i \mathbf{V}_i^H \mathbf{E}_i^H + N_0 \mathbf{I}_M. \quad (37)$$

Since the matrix FP reformulation expresses the objective through the matrices (23) and (24), it is sufficient to study how these quantities depend on the individual BD-RIS contributions.

From (35), the matrix \mathbf{A}_k admits the exact decomposition

$$\mathbf{A}_k = \sum_{b=0}^B \mathbf{A}_k^{(b)}, \quad \mathbf{A}_k^{(b)} \triangleq \mathbf{E}_k^{(b)H} \mathbf{Y}_k (\mathbf{I}_M + \mathbf{Z}_k). \quad (38)$$

Similarly, \mathbf{B}_k can be expanded exactly as

$$\mathbf{B}_k = \sum_{b=0}^B \sum_{c=0}^B \mathbf{B}_k^{(b,c)}, \quad \mathbf{B}_k^{(b,c)} \triangleq \mathbf{E}_k^{(b)H} \mathbf{Y}_k (\mathbf{I}_M + \mathbf{Z}_k) \mathbf{Y}_k^H \mathbf{E}_k^{(c)}. \quad (39)$$

Hence, all coupling among different BD-RISs appears only through the cross terms

$$\mathbf{B}_k^{(b,c)}, \quad b \neq c, \quad b, c \in \{1, \dots, B\}. \quad (40)$$

Assume now that the reflected contributions generated by different BD-RISs are weakly coupled in the sense that

$$\|\mathbf{B}_k^{(b,c)}\|_F \ll \|\mathbf{B}_k^{(b,b)}\|_F, \quad b \neq c, \quad b, c \in \{1, \dots, B\}, \quad (41)$$

for all k , which is reasonable when the deployed BD-RISs are sufficiently separated in space, induce sufficiently distinct angular signatures, or are optimized so that their reflected fields are weakly correlated at the users.

$$\nabla_{\Theta^{(b)}} \check{\eta} \approx \sum_{k \in \mathcal{K}} \left[\mathbf{H}_{\text{RX},k}^{(b)H} \mathbf{Y}_k (\mathbf{I}_M + \mathbf{Z}_k) \mathbf{V}_k^H \bar{\mathbf{H}}_{\text{TX}}^{(b)H} - \mathbf{H}_{\text{RX},k}^{(b)H} \mathbf{Y}_k (\mathbf{I}_M + \mathbf{Z}_k) \mathbf{Y}_k^H (\bar{\mathbf{H}}_k + \mathbf{H}_{\text{RX},k}^{(b)} \Theta^{(b)} \bar{\mathbf{H}}_{\text{TX}}^{(b)}) \left(\sum_{i \in \mathcal{K}} \mathbf{V}_i \mathbf{V}_i^H \right) \bar{\mathbf{H}}_{\text{TX}}^{(b)H} \right] \quad (48)$$

Finally, (39) can be rewritten as

$$\mathbf{B}_k = \mathbf{B}_k^{(0,0)} + \sum_{b=1}^B \mathbf{B}_k^{(0,b)} + \sum_{b=1}^B \mathbf{B}_k^{(b,0)} + \sum_{b=1}^B \mathbf{B}_k^{(b,b)} + \sum_{b=1}^B \sum_{\substack{c=1 \\ c \neq b}}^B \mathbf{B}_k^{(b,c)}, \quad (42)$$

where under (41), the matrix \mathbf{B}_k is approximated as

$$\mathbf{B}_k \approx \mathbf{B}_k^{(0,0)} + \sum_{b=1}^B \left(\mathbf{B}_k^{(0,b)} + \mathbf{B}_k^{(b,0)} + \mathbf{B}_k^{(b,b)} \right), \quad (43)$$

that is, the direct-path terms and the terms involving only the b -th BD-RIS are retained, whereas the terms coupling different BD-RISs are neglected.

Substituting (38) and (43) into the reformulated objective

$$\check{\eta}_k = 2 \text{Tr} \left(\Re \left\{ \mathbf{V}_k^H \mathbf{A}_k \right\} \right) - \text{Tr} \left(\sum_{i \in \mathcal{K}} \mathbf{V}_i \mathbf{V}_i^H \mathbf{B}_k \right), \quad (44)$$

yields

$$\check{\eta}_k \approx \check{\eta}_k^{(0)} + \sum_{b=1}^B \check{\eta}_k^{(b)}, \quad (45)$$

where $\check{\eta}_k^{(0)}$ is independent of $\{\Theta^{(b)}\}_{b=1}^B$ and

$$\check{\eta}_k^{(b)} \triangleq 2 \text{Tr} \left(\Re \left\{ \mathbf{V}_k^H \mathbf{A}_k^{(b)} \right\} \right) - \text{Tr} \left(\sum_{i \in \mathcal{K}} \mathbf{V}_i \mathbf{V}_i^H \left(\mathbf{B}_k^{(0,b)} + \mathbf{B}_k^{(b,0)} + \mathbf{B}_k^{(b,b)} \right) \right). \quad (46)$$

Therefore, the approximate contribution of the b -th BD-RIS depends only on

$$\mathbf{E}_k^{(b)} \triangleq \mathbf{H}_{\text{RX},k}^{(b)} \Theta^{(b)} \bar{\mathbf{H}}_{\text{TX}}^{(b)}, \quad (47)$$

and on the direct channel $\bar{\mathbf{H}}_k$, but not on the channels of any other BD-RIS.

Consequently, the gradient of the approximate objective with respect to $\Theta^{(b)}$ depends only on the local CSI of the b -th BD-RIS. In particular, by keeping only the terms in (46) that depend on $\Theta^{(b)}$, the gradient is obtained, as shown at the top of this page of the article, as seen in (48).

It has been shown that, after neglecting the inter-BD-RIS coupling terms $\mathbf{B}_k^{(b,c)}$ for $b \neq c$, the passive update of the b -th BD-RIS depends only on the channels incident on that surface, and the channels from that surface to the users, $\bar{\mathbf{H}}_{\text{TX}}^{(b)}$ and $\mathbf{H}_{\text{RX},k}^{(b)}$, respectively, together with the direct channel term $\bar{\mathbf{H}}_k$ when the latter is retained. Therefore, the channels associated with the remaining BD-RISs can be neglected in the passive update of $\Theta^{(b)}$.

REFERENCES

- [1] E. Björnson, H. Wymeersch, B. Matthiesen, P. Popovski, L. Sanguinetti, and E. de Carvalho, "Reconfigurable intelligent surfaces: A signal processing perspective with wireless applications," *IEEE Signal Processing Magazine*, vol. 39, no. 2, pp. 135–158, 2022.
- [2] Y. Liu, X. Liu, X. Mu, T. Hou, J. Xu, M. D. Renzo, and N. Al-Dahir, "Reconfigurable intelligent surfaces: Principles and opportunities," *IEEE Commun. Surveys Tuts.*, vol. 23, no. 3, pp. 1546–1577, 2021.
- [3] M. Nerini, S. Shen, and B. Clerckx, "Closed-form global optimization of beyond diagonal reconfigurable intelligent surfaces," *IEEE Transactions on Wireless Communications*, 2023.
- [4] M. Fidanovski, I. A. M. Sandoval, K. R. R. Ransinghe, G. T. F. de Abreu, E. Björnson, and B. Clerckx, "Fractional programming and manifold optimization for reciprocal BD-RIS scattering matrix design," 2025. [Online]. Available: <https://arxiv.org/abs/2511.07683>
- [5] M. Fidanovski, I. A. M. Sandoval, H. S. Rou, G. T. F. de Abreu, and E. Björnson, "Reciprocal beyond-diagonal reconfigurable intelligent surface (BD-RIS): Scattering matrix design via manifold optimization," 2026. [Online]. Available: <https://arxiv.org/abs/2509.20246>
- [6] E. Björnson, M. Bengtsson, and B. Ottersten, "Optimal multiuser transmit beamforming: A difficult problem with a simple solution structure [lecture notes]," *IEEE Signal Processing Magazine*, vol. 31, no. 4, pp. 142–148, 2014.
- [7] A. B. Gershman, N. D. Sidiropoulos, S. Shahbazpanahi, M. Bengtsson, and B. Ottersten, "Convex optimization-based beamforming," *IEEE Signal Processing Magazine*, vol. 27, no. 3, pp. 62–75, 2010.
- [8] L. C. Godara, *Handbook of antennas in wireless communications*. CRC press, 2018.
- [9] H. Li, S. Shen, Y. Zhang, and B. Clerckx, "Channel estimation and beamforming for beyond diagonal reconfigurable intelligent surfaces," *IEEE Transactions on Signal Processing*, vol. 72, pp. 3318–3332, 2024.
- [10] H. Li, S. Shen, and B. Clerckx, "Beyond diagonal reconfigurable intelligent surfaces: A multi-sector mode enabling highly directional full-space wireless coverage," *IEEE Journal on Selected Areas in Communications*, vol. 41, no. 8, pp. 2446–2460, 2023.
- [11] Z. Liu, Y. Liu, S. Shen, Q. Wu, and Q. Shi, "Enhancing ISAC network throughput using beyond diagonal RIS," *IEEE Wireless Communications Letters*, vol. 13, no. 6, pp. 1670–1674, 2024.
- [12] K. Chen and Y. Mao, "Transmitter side beyond-diagonal RIS for mmwave integrated sensing and communications," in *2024 IEEE 25th International Workshop on Signal Processing Advances in Wireless Communications (SPAWC)*, 2024, pp. 951–955.
- [13] Y. Zhou, Y. Liu, H. Li, Q. Wu, S. Shen, and B. Clerckx, "Optimizing power consumption, energy efficiency, and sum-rate using beyond diagonal RIS—a unified approach," *IEEE Transactions on Wireless Communications*, vol. 23, no. 7, pp. 7423–7438, 2024.
- [14] H. Li, S. Shen, and B. Clerckx, "Beyond diagonal reconfigurable intelligent surfaces: From transmitting and reflecting modes to single-, group-, and fully-connected architectures," *IEEE Transactions on Wireless Communications*, vol. PP, pp. 1–1, 01 2022.
- [15] M. Grant and S. Boyd, "CVX: Matlab software for disciplined convex programming, version 2.1," <https://cvxr.com/cvx>, Mar. 2014.
- [16] Z. Wu and B. Clerckx, "Optimization of beyond diagonal RIS: A universal framework applicable to arbitrary architectures," 2024. [Online]. Available: <https://arxiv.org/abs/2412.15965>
- [17] T. Fang and Y. Mao, "A low-complexity beamforming design for beyond-diagonal RIS aided multi-user networks," *IEEE Communications Letters*, vol. 28, no. 1, pp. 203–207, 2024.
- [18] X. Xu, Y. Ju, Z. Li, X. Hou, L. Liu, S. Mumtaz, and C. Wu, "Beamforming design for multi-sector BD-RIS assisted FL with aircomp," in *2025 IEEE Wireless Communications and Networking Conference (WCNC)*, 2025, pp. 1–6.
- [19] E. Björnson, L. Sanguinetti, H. Wymeersch, J. Hoydis, and T. L. Marzetta, "Massive MIMO is a reality—what is next?: Five promising research directions for antenna arrays," *Digital Signal Processing*, vol. 94, pp. 3–20, 2019, special Issue on Source Localization in

- Massive MIMO. [Online]. Available: <https://www.sciencedirect.com/science/article/pii/S1051200419300776>
- [20] X. Ma, D. Zhang, M. Xiao, C. Huang, and Z. Chen, "Cooperative beamforming for RIS-aided cell-free massive MIMO networks," *IEEE Transactions on Wireless Communications*, vol. 22, no. 11, pp. 7243–7258, 2023.
- [21] M. Liu, M. Li, R. Liu, and Q. Liu, "Distributed distortion-aware beamforming designs for cell-free mMIMO systems," *IEEE Journal of Selected Topics in Signal Processing*, 2025.
- [22] K. D. Katsanos and G. C. Alexandropoulos, "Decentralized cooperative beamforming for BDRIS-assisted cell-free MIMO OFDM systems," 2026. [Online]. Available: <https://arxiv.org/abs/2601.13201>
- [23] S. Shi, S. Zhu, X. Gu, and R. Hu, "Extendable carrier synchronization for distributed beamforming in wireless sensor networks," in *2016 International Wireless Communications and Mobile Computing Conference (IWCMC)*, 2016, pp. 298–303.
- [24] A. Ghani, H. Naqvi, M. S. Ramzan, M. Khattak, I. Khan, and A. Irshad, "Spread spectrum based energy efficient collaborative communication in wireless sensor networks," *PLOS ONE*, vol. 11, p. e0159069, 07 2016.
- [25] J. Pearce, "Limiting liability with positioning to minimize negative health effects of cellular phone towers," *Environmental Research*, vol. 181, p. 108845, 2020. [Online]. Available: <https://www.sciencedirect.com/science/article/pii/S0013935119306425>
- [26] C. Roda and S. Perry, "Mobile phone infrastructure regulation in europe: Scientific challenges and human rights protection," *Environmental Science and Policy*, vol. 37, pp. 204–214, 2014. [Online]. Available: <https://www.sciencedirect.com/science/article/pii/S146290111300186X>
- [27] K. Shen, "Fractional programming for communication system design," Ph.D. dissertation, Stanford University, 2018, ph.D. dissertation, available online. [Online]. Available: https://kaimingshen.github.io/doc/shen_thesis.pdf
- [28] K. Shen and W. Yu, "Fractional programming for communication systems—part I: Power control and beamforming," *IEEE Transactions on Signal Processing*, vol. 66, no. 10, pp. 2616–2630, May 2018.
- [29] —, "Fractional programming for communication systems—part II: Uplink scheduling via matching," *IEEE Transactions on Signal Processing*, vol. 66, no. 10, pp. 2631–2644, 2018.
- [30] I. Sandoval, K. Ando, O. Taghizadeh, and G. Abreu, "Sum-rate maximization and leakage minimization for multi-user cell-free massive MIMO systems," *IEEE Access*, vol. PP, pp. 1–1, 01 2023.
- [31] 3GPP, "Further advancements for E-UTRA physical layer aspects," 3rd Generation Partnership Project (3GPP), Technical Report TR 36.814, Mar. 2017.
- [32] L. Miretti, R. L. G. Cavalcante, E. Björnson, and S. Stańczak, "UL-DL duality for cell-free massive MIMO with per-AP power and information constraints," *IEEE Transactions on Signal Processing*, vol. 72, pp. 1750–1765, 2024.